Brazilian Dental Science

unesp
UNIVERSIDADE ESTADUAL PAULISTA
"JÚLIO DE MESQUITA FILHO"
Instituto de Ciência e Tecnologia
Campus de São José dos Campos

ORIGINAL ARTICLE

DOI: https://doi.org/10.4322/bds.2022.e3488

Characterization of sound enamel and natural white spot lesions

Caracterização de esmalte hígido e lesões de mancha branca naturais

Erika Michele dos Santos ARAUJO[1], Cristina de Mattos Pimenta VIDAL[2], Anderson Zanardi de FREITAS[3], Niklaus Ursus WETTER[3], Adriana Bona MATOS[1]

1 - Universidade de São Paulo, Faculdade de Odontologia, Departamento de Dentística, São Paulo, SP, Brazil.
2 - University of Iowa, College of Dentistry, Department of Operative Dentistry, Iowa City, IA, USA.
3 - Instituto de Pesquisas Energéticas e Nucleares, São Paulo, SP, Brazil.

ABSTRACT

Objective: To compare optical, morphological, chemical, and physical aspects of the sound enamel and white spot lesions (WSL) classified as ICDAS 2. **Material and Methods:** Seventeen human molars with one surface presenting WSL and a sound surface (2 x 2 mm window) were characterized by Quantitative light-induced fluorescence (QLF®), Optical coherence tomography (OCT), microhardness, and Raman spectroscopy. The ANOVA and Tukey's test were used at 5% significance level. **Results:** The QLF comparison between distinct substrates yielded decreased ΔQ (integrated fluorescence loss) of -15,37%mm^2 and -11,68% ΔF (fluorescence loss) for WSL. The OCT detected mean lesion depth of 174,43 μm. ANOVA could not detect differences in the optical attenuation coefficient between the substrates ($p>0.05$). Lower microhardness measures were observed in WSL than on sound enamel ($p<0.05$). The Raman spectra showed four vibrational phosphate bands ($v1$, $v2$, $v3$, $v4$), where the highest peak was at 960.3 cm^{-1} ($v1$) for both substrates. However, a 40% decrease in phosphate ($v1$) was detected in WSL. The peak at 1071 cm^{-1} was higher for sound enamel, indicating the presence of a phosphate band instead of the B-type carbonate. The spectra showed higher intensity of the organic composition at 1295 cm^{-1} and 1450 cm^{-1} for WSL. **Conclusion:** Non-invasive QLF, OCT and Raman spectroscopy were able to distinguish differences in fluorescence, optical properties, and organic/inorganic components, respectively, between sound enamel and WSL, validated by the destructive microhardness analysis.

KEYWORDS

Dental caries; Dental enamel; White-spot lesions; Diagnosis; Raman Spectroscopy.

RESUMO

Objetivo: Comparar os aspectos ópticos, morfológicos, químicos e físicos do esmalte sadio e das lesões de mancha branca naturais, classificada como ICDAS 2. **Material e métodos:** Dezessete molares humanos com uma face apresentando uma lesão de mancha branca natural e outra face o esmalte hígido (2 x 2 mm) foram caracterizados utilizando a Fluorescência quantitativa induzida pela luz (QLF®), Tomografia de coerência óptica (OCT), Microdureza e Espectroscopia Raman. A ANOVA e o teste de Tukey foram utilizados ao nível de significância de 5%. **Resultados:** A comparação entre os substratos distintos, utilizando o QLF® demonstrou uma diminuição no ΔQ (perda de fluorescência integrada) de -15,37%mm^2 e -11,68% de ΔF (Perda de fluorescência) para a lesão de mancha branca. O OCT detectou uma profundidade média de lesão de 174,43μm. A ANOVA não detectou diferenças no coeficiente de atenuação óptica entre os substratos (>0,05). Microdureza significantemente menor foi detectada nas lesões de mancha branca do que no esmalte sadio ($p<0,05$). Os espectros Raman mostraram quatro bandas vibracionais do fosfato (v1, v2,v3,v4), onde o maior pico foi em 960,3cm^{-1} para ambos os substratos. No entanto, uma diminuição de 40% no fosfato (v1) foi detectada na lesão. O pico em 1071cm^{-1} foi maior para o esmalte hígido, demonstrando tratar-se da banda do fosfato, ao invés do carbonato tipo B. Os espectros apresentaram maior intensidade da composição orgânica em 1295cm^{-1} e 1450 cm^{-1} para a lesão de mancha branca. **Conclusão:** Os métodos não invasivos QLF, OCT e espectroscopia Raman foram capazes de

diferenciar a fluorescência, propriedades ópticas e conteúdo orgânico/inorgânico do esmalte sadio comparado com esmalte com lesões de mancha branca, sendo validado pela análise de microdureza.

PALAVRAS-CHAVE:

Cárie dental; Esmalte dental; Lesão de mancha branca; Diagnóstico; Espectroscopia Raman.

INTRODUCTION

The early diagnosis of enamel caries lesions in their subclinical stage is still a great challenge for clinicians and researchers. Therefore, the use of multiple caries diagnostic tools and their association are desirable to help dentists during their clinical routine. A precise early diagnose is essential to control and prevent the progression of the disease by implementing minimally invasive strategies.

It is well known that the deposition of dental biofilm on the enamel surface, the inefficiency of its removal, and the frequent intake of fermentable carbohydrates predispose the initial caries lesions development [1]. The organic acids penetrate the dental enamel, partially dissolve the hydroxyapatite crystals and lead to the loss of calcium and phosphate [1]. This phenomenon may be delayed or paralyzed by saliva, which acts towards mineral deposition and pH increase [1]. Hence, lesion formation is a dynamic process in which the remineralization by saliva makes the environment less critical for the balance of dental structure [1], and the demineralization can be paralyzed; thus, the surface will recrystallize [2-4].

In this context, the minimally invasive dentistry seeks for early diagnostic tools to implement management of lesions at their initial stage. Clinical treatment options for active WSLs have shown to be highly successful, promoting lesion arrest and avoiding cavitation and can include fluoride-containing toothpaste, varnishes, and restorative materials [5]. In some cases, esthetic micro-invasive or minimally invasive procedures can mask the white appearance of those lesions [6]. However, the development and improvement of different treatment options rely on understanding how caries initiation affects enamel to better predict clinical outcomes. In addition, predicting the performance of in vitro treatments in clinical lesions can be challenging since artificial lesions may not present the same optical, chemical, and mechanical characteristics as the sound enamel. Understanding the particularities of white spot lesions is essential to indicate the best treatment [7], and it will directly influence the reproducibility and reliability on in situ and in vivo studies.

Visual clinical examination is the conventional diagnostic tool used worldwide, routinely refined using magnification and proper illumination. But when doubts arise, the association of the visual exam with other caries diagnostic tools could improve diagnostic precision [8,9] of enamel lesions in its early stages. Non-invasive methods, such as Quantitative Light-induced fluorescence (QLF) that analyzes enamel autofluorescence comparing sound and demineralized areas [10-12]; Optical Coherence Tomography, which scans the caries lesions, determines their depths, birefringence and the attenuation coefficient of the light inside the substrate that quantifies the interaction between light and the components inside the analyzed substrates [13-17]; and chemical analysis using Raman spectroscopy [9,18-22] that provides information regarding changes in the inorganic and organic component of substrates could act as extra strategies in caries diagnosis. To validate these non-invasive above mentioned methods, microhardness was proposed as it is well known to easily distinguish between sound and carious enamel [23-27] especially subclinical lesions. With this rationale, this study aimed to evaluate optical, morphological, chemical, and physical features of enamel surface with WSL and compare them with sound enamel. The null hypothesis tested was: There would be no difference between the characteristics of the sound enamel and WSL analyzed.

MATERIAL AND METHODS

Seventeen human molars were obtained from the Biobank of Human Teeth at the University of Sao Paulo, School of Dentistry, following a protocol approved by the Local Ethics Committee (#3.742.709). As inclusion criteria, the teeth should present a surface (smooth or proximal) with a natural WSL classified as ICDAS 2 and

sound enamel on its homologous surface. The teeth were cleaned and then stored without any solution in a refrigerator at 4ºC until use.

Before using the teeth for the different methods described, the lesions' size was evaluated, and a reading window (2 × 2 mm) on both the WSL and sound enamel surfaces was standardized using adhesive tape.

Quantitative light-induced fluorescence (QLF)

The teeth were dried for 10 s using a triple syringe immediately before the readings and positioned perpendicularly to the QLF handpiece, and focused. A single examiner performed all the QLF readings, and the images were analyzed using the QLF software (Inspektor Research System BV, Amsterdam, The Netherlands). Differences in fluorescence (ΔF) and integrated fluorescence loss (ΔQ = ΔF by lesion area) values were recorded at a threshold level of 5%, so 95% of fluorescence loss between sound enamel and the white spot lesion were detected. Data collected included average fluorescence loss expressed in percentage (ΔF*)*, size of the WSL area (mm^2), and difference in fluorescence integrated by lesion area (ΔQ), expressed -$\%mm^2$.

Optical Coherence Tomography (OCT) - Lesion depth and Optical attenuation coefficient

The teeth were examined by OCT using a superluminescent LED operated at 930 nm with 2mW of power (OCP930RS Thorlabs Inc.), with an axial resolution of 4 μm, the lateral resolution of 6 μm and considering a refractive index of 1.6, for human enamel. Images were acquired and used to determine the lesion depth and the optical attenuation coefficient.

Lesion depth was evaluated using the software Image J (NIH) to calculate lesion depth. The lesions were analyzed by scanning them along five horizontal lines, separated by 300μm, and analyzing the image with the software. The mean of the lesion depth (in μm) on the five lines was determined for each surface.

The total optical attenuation coefficient obtained from 5 images per sample was analyzed using homemade software developed in LabView 8. The coefficient was calculated assuming an exponential decay of light intensity inside enamel and lesion (backscattered), according to the Equation 1:

$$I(z) = I_0 e^{-\alpha z} + C \quad (1)$$

Where: *I(z)* represents detected in-depth intensity z; I_0 is the source intensity value at the sample surface; α is the whole optical attenuation coefficient; z is the evaluated depth; and C is a constant to reduce background noise signal [16]. The arithmetic mean for five values of the attenuation coefficient was obtained for each sample.

Cross-sectional microhardness analysis

After the non-invasive QLF and OCT measurements, dental roots were removed 2 mm below the root crown junction in each tooth, and the crown was vertically sectioned in the buccal-lingual or mesio-distal direction. After that, samples were sequentially polished with silicon carbide papers (P1200 for 30 s, P2500 for 30 s, and P4000 for 4 min) and ultra-sonicated between each abrasive paper for 5 min [28]. The opposite surface was also polished to obtain a flat surface, an indispensable requirement for microhardness measurements using a microhardness Knoop indenter (HMV-G21DT, Shimadzu Co., Tokyo, Japan). A 25 g load was used for 10 s to produce a diamond-shaped indentation under 40 x magnification [23]. Measurements were performed as shown in Figure 1. On each cross-section from the area near the enamel surface (Surface layer- SL) (between 30-50 μm from outer enamel) until a sound enamel (SE), for WSL. For sound enamel, the same WSL reference was used, both following reference values for Knoop hardness. KHN (Knoop hardness number) results from all samples in each condition (sound or WSL) were averaged.

Raman spectroscopy

The chemical characterization of the sound enamel and WSLs (n=3) was performed using the LabRAM HR Evolution Raman spectrometer (HORIBA, Scientific France SAS, France). Samples were analyzed without any previous treatment (sectioning or polishing) using a wavelength of 633 nm, the laser power was 120mW, the pinhole was 200 μm, and 90 acquisitions of 1 s each were made using 0.7 cm^{-1} of spectral resolution (600 lines/mm grating), and a 10x objective [20].

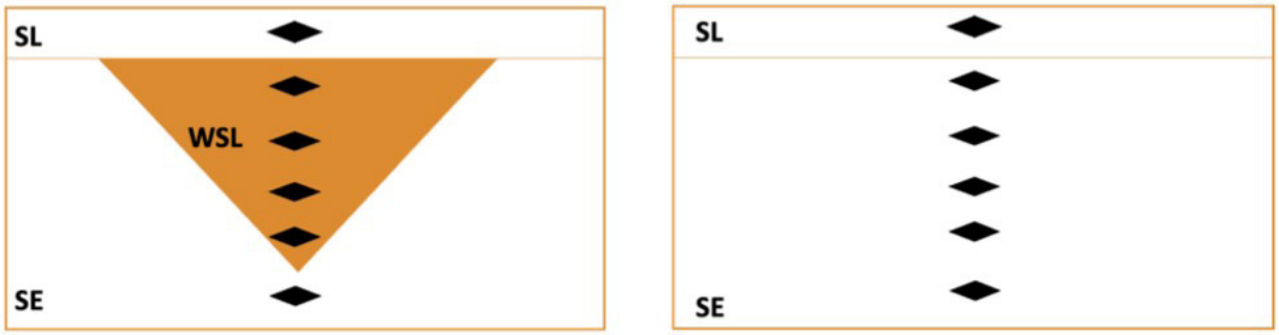

Figure 1 - Cross-sectional microhardness analysis for WSL and Sound enamel (SE).

The spectral range was fixed at 400-1500 cm^{-1} to analyze the inorganic and organic composition, namely phosphates, carbonates, and organic content. Additionally, photobleaching was performed using the maximum laser power for 5 min before all the readings. Three points were analyzed on sound enamel and three points on natural white spot lesion for each sample. After this, the spectra were processed with a baseline correction, normalized by mean, and smoothened by an 8-point third order polynomial, using LabSpec 6 software (HORIBA, Scientific France SAS, France). The chemical composition analysis was performed on the surface of the substrates, and the collected data were processed and normalized. The data normalization was done using the final average value of the entire spectra specified for each tooth.

Statistical analysis

QLF and Raman spectroscopy results were qualitatively described. One-way ANOVA or two-way ANOVA followed by Tukey's post hoc tests ($\alpha=0.05$) were conducted to compare sound enamel and WSLs for OCT and microhardness results, using the Minitab 9 software (Minitab Inc., State College, PA, USA).

RESULTS

The QLF data are described in Table I. The average ΔQ (-% mm^2) indicates loss of integrated fluorescence, when compared sound and demineralized areas, on the lesion size of -15%mm^2 (on average) of the total area analyzed. Therefore, the values of ΔQ described above have a high coefficient of variation. These values were calculated by multiplying the ΔF (fluorescence loss value) by the demineralized area (mm^2) WSL mean size was 1.4 mm^2 with a 71% variation in size within the different lesions. The difference in fluorescence between the sound enamel and the WSL was -11.68%.

Table I - Descriptive statistics of fluorescence loss obtained using the QLF®. ΔQ (integrated fluorescence loss, expressed in %mm^2, ΔF (fluorescence loss, expressed in percentage), and area (expressed in mm^2)

Parameters	Mean ± standard deviation (Coefficient of variation in %)
ΔQ (%mm^2)	-15.37 ± 14.78 (96.14)
Area (mm^2)	1.41 ± 0.74 (70.97)
ΔF (5%)	-11.68 ± 6.33 (54.20)

Regarding lesion depth, OCT was able to detect lesions between the range 240.70 to 115.74 μm, with an average lesion depth of 174.43 ± 7.52 μm, with a coefficient of variation of 17.25%.

One-way ANOVA demonstrated no significant difference between the values of the optical attenuation coefficient when comparing the sound enamel and the WSL region ($p > 0.05$) (Table II).

For the microhardness data (Table III), two-way ANOVA demonstrated a statistically significant difference between the substrates ($p < 0.001$), but similar results for location of the readings in the same sample (surface vs. cross-sectional) ($p > 0.05$) and no interaction between these two factors ($p > 0.05$). Additionally, comparisons were made between the surface layer (up to 50μm) and the other depths evaluated (100μm- 500μm), both for the sound enamel and the white spot lesion. For sound enamel, the comparison of the surface layer (50μm) vs. all the depths described above showed no significant difference ($p>0.01$). When the white spot lesion was evaluated, there was no significant difference between the microhardness of the surface layer

(up to 50μm) compared with all the other depths (100μm-500μm), ($p>0.01$).

The resultant spectra averages for all teeth in each condition (sound enamel and WSL) obtained with the Raman spectroscopy are shown in Figure 2. Regarding enamel's inorganic content, the highest peak is at 960.3 cm^{-1} ($v1$ PO_4) for both sound enamel and the WSL, with a 40% decrease in WSL compared to sound enamel. Peaks at 1052 cm^{-1} ($v3$ PO_4), 579 cm^{-1} ($v3$ PO_4), 431 cm^{-1} and 446 cm^{-1} ($v2$ PO_4) were also clearly seen, with higher values for the sound enamel when compared to the WSL. Higher peak intensity in the 1071 cm^{-1} ($v3$ PO_4) band was detected for the sound enamel than WSL. In addition, two other peaks were verified, 1295 cm^{-1} (amide III) and 1450 cm^{-1} (CH_2), which showed greater intensity on the WSLs than sound enamel.

Table II - Mean ± standard deviation of the optical attenuation coefficient (μm^{-1}) (n=17) for sound enamel and WSLs

Substrate	Mean ± Standard deviation (Coefficient of variation in %)
Sound enamel	1.500 ± 0.849 (56.61)[a*]
WSL	1.411 ± 0.495 (35.08) [a]

*Similar letters (column) represent no statistically significant difference ($p>0.05$).

DISCUSSION

This study compared sound enamel and WSLs in several aspects, including chemical composition, mechanical and optical properties. Overall, all properties are altered in WSLs compared to sound enamel, which led to the rejection of the null hypothesis. In addition, lesion depth and changes in mineral content at the lesion body were also evaluated.

As a method to evaluate the fluorescence, QLF® was used to analyze variations in the mineral content of the surface. The QLF is

Table III - Mean ± standard deviation (coefficient of variation in%) of KHN of sound enamel and WSL surface and cross-sectional/inner area (n=17)

Substrate (n=17)	Surface layer	Bottom of the lesion
Sound enamel	316.4 ± 73.9 (23.35)[a*]	328.54 ± 37.72 (11.48)[A*]
WSL	166.7 ± 94.5 (56.67)[b]	131.8 ± 56.6 (42.95)[B]

*Different superscript letters (column) represent statistically significant difference ($p < 0.05$).

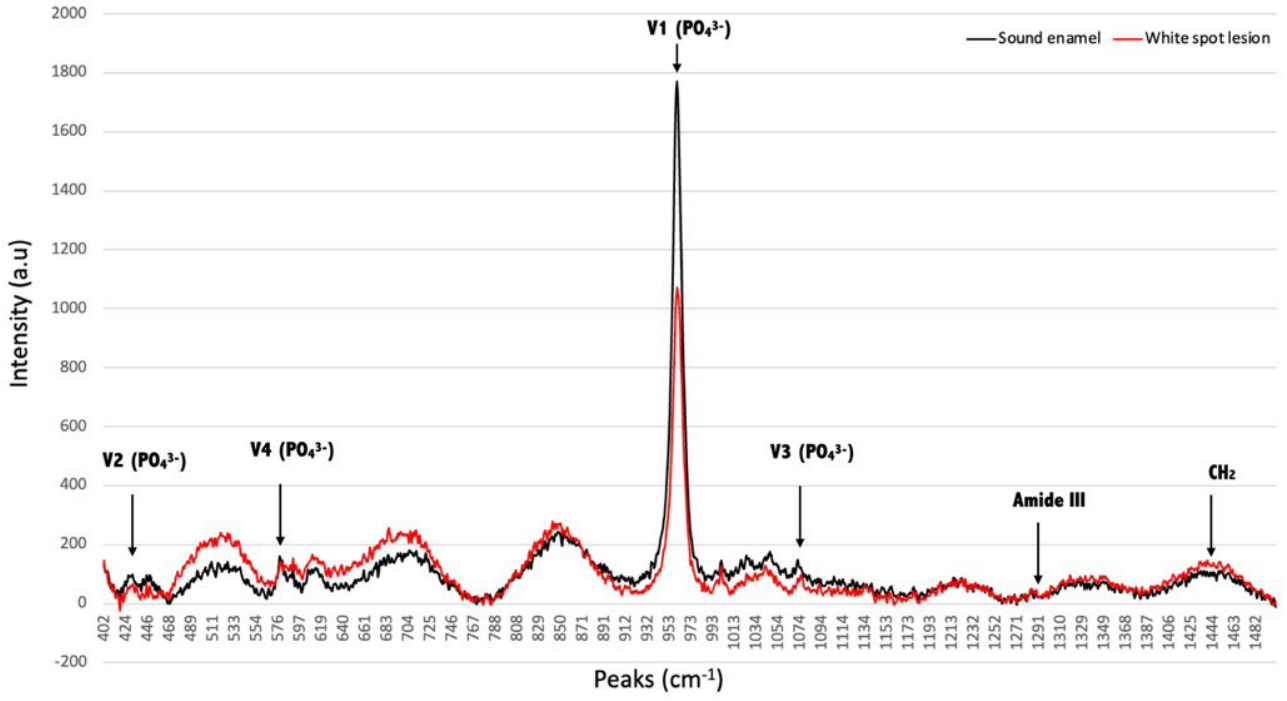

Figure 2 - The spectra average for all surfaces in each condition representing all the bands for sounds enamel and WSL. Arrows indicate peaks at 431cm^{-1}($v2$ PO_4), 579cm^{-1}($v3$ PO_4), 960cm^{-1} ($v1$ PO_4), 1071cm^{-1} ($v3$ PO_4) related to phosphate vibrational modes and 1295cm^{-1}(amide III), 1450cm^{-1} (CH_2), related to organic content.

used to diagnose early caries lesions, monitor them, and correlate mineral loss and loss of fluorescence [10,29]. This method compared the optical differences between sound and WSL, as an autofluorescence coming from its enamel-dentin junction [10-12,30]. In WSL, enamel autofluorescence decreases and can be attributed to the scattering effect, leading to less excitation of the substrate by the irradiated light or different emission from the excitation of the demineralized region [10,31,32].

In this study, the QLF was efficient in comparing the fluorescence of sound and WSL enamel. It showed a reduction of -15%mm^2 of integrated fluorescence loss (ΔQ) and -11.68% of fluorescence loss (Δ*F*) for WSLs. These values are related to mineral loss and to lesion depth, which presents a good correlation with changes in mineral content compared to methodologies such as microradiography [33]. It is noteworthy to mention that the loss of minerals was also evidenced in the Raman readings, which demonstrated a decrease of 40% in the phosphate peak (v1) intensity in WSL. This peak of the spectra is the symmetrical stretching mode of phosphate (v1) at 960.3cm-1, which is the highest peak related to mineralized tissues, such as enamel, dentin, and bone [9,18,19,21]. These results follow some studies demonstrating that decreased phosphate content indicates lower mineralization [9,19]. The enamel comprises hydroxyapatite Ca10(PO4)6(OH)2 crystals and other ions, such as carbonate. This study showed that the phosphate vibration modes (v1, v2, v3, and v4), presented higher intensity in sound enamel due to a more significant amount of phosphate on this surface [19] when compared to WSL.

The QLF® is a clinical diagnostic tool that has been used in laboratorial studies [10] to monitor the effect of different dental materials and treatments in incipient artificial lesions. Therefore, by understanding QLF parameters (fluorescence loss and the loss of integrated fluorescence) of natural lesions could help standardize the development of artificial lesions for future studies.

As a limitation of this method, we observed a high coefficient of variation of ΔQ; it is likely due to the variation of the demineralized areas captured. The natural WSL inherently vary in size and depth, thus this variation was expected and confirmed by the OCT results that detected lesion depths from 116 μm to 241 μm.

Several studies have been carried out using the OCT to diagnose incipient caries due to the optical properties that are altered after the demineralization process [34-37]. The OCT measures the optical attenuation coefficient, a parameter that quantifies the interaction between light and the components inside the analyzed substrates (A-scan). For this purpose, graphics obtained from OCT readings were analyzed based on the first peak referring to the change in light reflectivity when it contacts the dental enamel surface and the subsequent extinction of this signal resulting in a value described in the results section [15,16,32,38]. In this study, the optical attenuation coefficient observed in sound enamel and WSL were similar. The literature presents controversial results for demineralized enamel compared to sound enamel. While some studies [16,32] detected higher attenuation coefficient values and a high degree of sensitivity and specificity using artificial caries lesions, others reported a lower optical attenuation coefficient for natural WSLs than sound enamel [15,38]. The higher value presented by WSL is due to prism disorganization and enlargement of pores in dental enamel [32]. Tissue disorganization and pores inside the substrate increase the number of interfaces with which the light will interact, increasing the scattering of light and, consequently, the value of the coefficient [16,32]. However, other studies [15,38] suggest that the more significant demineralization presented by natural lesions leads to a greater loss of minerals and larger porosities that can increase the probability that the light does not interact with any structure (light scattering centers) inside the enamel, so light scattering on the tissue will decrease [38]. In this study, the intrinsic size variability of the WSL demonstrated above may be responsible for not detecting differences in the attenuation coefficient between sound enamel and WSL.

Moreover, our Raman results detected a peak in the 1295 cm-1 band which is related to the presence of proteins, such as amelogenin, in the pores of enamel crystallites [9]. Alike Sadyrin [9], we observed a peak in this region, which corresponds with amide III (= CH) [19]. Although the amount of organic content of enamel is not comparable to inorganic content, the enlargement of enamel pores after the

demineralization of this substrate can account for protein and lipid content in dental enamel [39].

The OCT was used to measure the lesion depth that yielded an average depth of 174.42 μm, within the estimated value for white spot lesions without a clinically visible appearance. Studies [29,40] indicated that initial caries lesions in enamel are visible to the naked eye when they reach a depth between 300-500μm. Interestingly, even though the deepest lesion detected with OCT in this study was 241 μm, when the microhardness analysis was performed, it was possible to verify changes in the KHN until around 500 μm from the lesion surface. The OCT device has a depth range of up to 1 mm, and this value may decrease after years of use [15]. In this way, the amount of light can be insufficient to penetrate the evaluated lesions in-depth, resulting in scattering light by the surface. In addition, factors such as the absorption coefficient and the interaction between the tissue and the wavelength may have decreased light penetration depth [15,38].

After the use of non-invasive methods use (QLF, OCT and Raman spectroscopy), a cross-sectional microhardness analysis was performed to validate differences between sound enamel and WSLs. As mentioned in the methodology, literature [41] previously defined that the reference value used for sound enamel is between 272 and 404 KHN. This study showed that the mean value of the sound enamel was inside this range, and the value for WSLs was significantly lower, demonstrating the demineralization of the substrate, which was also observed by the decrease of 40% in the phosphate peak (v1) intensity in WSL using Raman. When comparing the KHN near the enamel surface (first reading at 30 to 50μm) for the two substrates, a 52% difference was observed. However, no difference was observed when superficial and bottom readings were compared in each substrate. It is worth mentioning that, as in the study by Craig and Peyton [42], our study carried out indentations on the longitudinal surface apart from studies such as Caldwell [23], which found greater hardness for the enamel surface layer.

The surface hardness analysis of the enamel is indicated when it evaluates artificial caries lesions, which commonly present a smaller demineralization depth. However, longitudinal hardness measurements are more indicated to evaluate the natural lesions with a higher depth [43]. While studies [44,45] reported that the surface/outer layer of enamel has a greater hardness than the inner enamel (body), it was not observed in our study that observed similar hardness values for surface layer and enamel body lesion, following Craig and Peyton [42]. This discrepancy might be related to the variation in the direction of indentations within the same tooth [46]. However, one study [45] stated that orientation does not directly influence hardness values. Therefore, in this study, all indentations were carried out parallel to the enamel surface. Moreover, enamel hardness varies from the enamel surface to the adjacent amelo-dentinal junction [47] due to a variation of the organic and inorganic content in dental enamel. In general, the enamel surface presents greater mineral content related to dynamic ionic exchanges with the oral cavity, while deeper regions are composed of greater organic content [48-50]. Interestingly, these differences were not detected for sound enamel or white spot lesions in this study when performed the microhardness analysis. We believe that the small size of the enamel lesions classified as ICDAS 2 included in this study could account for the absence of differences in microhardness values.

Regarding the Raman spectroscopy readings, in addition to a decrease in the phosphate peak (v1) and the detection of the presence of organic content (amide III) in WSLs, it was possible to observe the peak of 1071 cm-1, referred to as phosphate v3 vibration mode and B-type carbonate [20,21]. To clarify, if this band represents carbonate or phosphate, observation of other bands is required. If other phosphate vibrations are expressed, then it is phosphate. On the other hand, if A-type carbonate is expressed in 1104 cm-1, the vibration in 1071 cm-1 can represent B-type carbonate. As other phosphate vibrations were expressed in this study, we consider that it represents phosphate (v3), with a higher vibration for sound enamel than for WSL [9,19].

It is known that the analyzed surface, although not intact, still has a high amount of phosphate because the demineralization process of WSL is initial and does not occur homogeneously, which could be observed in Raman results. Also, in deeper lesions, the carbonate substitution of phosphate in the apatite lattice can occur [20,21,28,51],

creating carbonated hydroxyapatite that is more susceptible to acid demineralization and responsible for the crystallographic changes of the prismatic structure. A previous study that analyzed mineralized substrates [52] found a band overlap of carbonate under the phosphate band, which did not occur in this study.

One of the limitations of this study relies on sample size and specific knowledge of the origin of the tooth. However, most of the non-invasive methods were able to distinguish sound enamel from WSL. This characterization is crucial for revisiting those substrates' essential aspects and characteristics and further developing enamel caries-like lesions, constructing a substrate that mimics natural lesions, and enabling innovative materials and therapeutic strategies.

CONCLUSION

Non-invasive QLF, OCT and Raman spectroscopy were able to distinguish differences in fluorescence, optical properties, and organic/inorganic components, respectively, between sound enamel and WSL. These results were validated by the destructive microhardness analysis. Future investigations should continue to explore the tissue properties, mainly from the subclinical incipient enamel lesion to the white spot lesion.

Acknowledgements

We thank Capes Foundation, Ministry of Education of Brazil, Brasília – DF, Brazil, zip code 70.040-020 (CAPES–process #88882.376626/2019-01 and #88887.371119/2019-00) for the financial support.

Author's Contributions

EMSA: Conceptualization, Investigation, Data curation, Writing - Original Draft. CMPV: Investigation, Data Curation, Writing - Original Draft. AZF: Methodology, Formal analysis, Writing - Review & Editing. NUW: Methodology, Data curation, Writing - Review & Editing. ABM: Supervision, Conceptualization, Resources, Formal analysis, Writing - Review & Editing.

Conflict of Interest

The authors have no proprietary, financial, or other personal interest of any nature or kind in any product, service, and/or company that is presented in this article.

Funding

Ministry of Education of Brazil, Brasília – DF, Brazil, zip code 70.040-020 (CAPES – process #88882.376626/2019-01 and #88887.371119/2019-00) for the financial support.

Regulatory Statement

This research was approved by the Local Ethics Committee of the University of Sao Paulo, School of Dentistry (#3.742.709).

REFERENCES

1. Robinson C, Shore RC, Brookes SJ, Strafford S, Wood SR, Kirkham J. The chemistry of enamel caries. Crit Rev Oral Biol Med. 2000;11(4):481-95. http://dx.doi.org/10.1177/10454411000110040601. PMid:11132767.
2. ten Cate JM, Arends J. Remineralization of artificial enamel lesions in vitro: III. A study of the deposition mechanism. Caries Res. 1980;14(6):351-8. http://dx.doi.org/10.1159/000260477. PMid:6933007.
3. Fejerskov O, Nyvad B, Kidd E. Dental caries: the disease and its clinical management. 3rd ed. Oxford: Wiley-Blackwell; 2015. Chap. 9.
4. Richards A, Larsen MJ, Fejerskov O, Thylstrup A. Fluoride content of buccal surface enamel and its relation to dental caries in children. Arch Oral Biol. 1977;22(7):425-8. http://dx.doi.org/10.1016/0003-9969(77)90122-4. PMid:271485.
5. Abdullah Z, John J. Minimally invasive treatment of white spot lesions--a systematic review. Oral Health Prev Dent. 2016;14(3):197-205. http://dx.doi.org/10.3290/j.ohpd.a35745. PMid:26973988.
6. Featherstone JD. Prevention and reversal of dental caries: role of low level fluoride. Community Dent Oral Epidemiol. 1999;27(1):31-40. http://dx.doi.org/10.1111/j.1600-0528.1999.tb01989.x. PMid:10086924.
7. Huang TT, Jones AS, He LH, Darendeliler MA, Swain MV. Characterisation of enamel white spot lesions using X-ray micro-tomography. J Dent. 2007;35(9):737-43. http://dx.doi.org/10.1016/j.jdent.2007.06.001. PMid:17683844.
8. Lippert F, Parker DM, Jandt KD. In vitro demineralization/remineralization cycles at human tooth enamel surfaces investigated by AFM and nanoindentation. J Colloid Interface Sci. 2004;280(2):442-8. http://dx.doi.org/10.1016/j.jcis.2004.08.016. PMid:15533417.
9. Sadyrin E, Swain M, Mitrin B, Rzhepakovsky I, Nikolaev A, Irkha V, et al. Characterization of enamel and dentine about a white spot lesion: mechanical properties, mineral density, microstructure and molecular composition. Nanomaterials (Basel). 2020;10(9):1889. http://dx.doi.org/10.3390/nano10091889. PMid:32967152.

10. Pretty IA. Caries detection and diagnosis: novel technologies. J Dent. 2006;34(10):727-39. http://dx.doi.org/10.1016/j.jdent.2006.06.001. PMid:16901606.

11. Gomez J, Pretty IA, Santarpia RP 3rd, Cantore B, Rege A, Petrou I, et al. Quantitative light-induced fluorescence to measure enamel remineralization in vitro. Caries Res. 2014;48(3):223-7. http://dx.doi.org/10.1159/000354655. PMid:24481051.

12. Gokce G, Savas S, Kucukyilmaz E, Veli I. Effects of toothpastes on white spot lesions around orthodontic brackets using quantitative light-induced fluorescence (QLF): an in vitro study. J Orofac Orthop. 2017;78:480-6. http://dx.doi.org/10.1007/s00056-017-0106-0.

13. Amaechi BT, Podoleanu A, Higham SM, Jackson DA. Correlation of quantitative light-induced fluorescence and optical coherence tomography applied for detection and quantification of early dental caries. J Biomed Opt. 2003;8(4):642-7. http://dx.doi.org/10.1117/1.1606685. PMid:14563202.

14. Ko AC, Choo-Smith LP, Hewko M, Leonardi L, Sowa MG, Dong CC, et al. Ex vivo detection and characterization of early dental caries by optical coherence tomography and Raman spectroscopy. J Biomed Opt. 2005;10(3):031118. http://dx.doi.org/10.1117/1.1915488. PMid:16229643.

15. Sowa MG, Popescu DP, Friesen JR, Hewko MD, Choo-Smith LP. A comparison of methods using optical coherence tomography to detect demineralized regions in teeth. J Biophotonics. 2011;4(11-12):814-23. http://dx.doi.org/10.1002/jbio.201100014. PMid:22052833.

16. Cara ACB, Zezell DM, Ana PA, Maldonado EP, Freitas AZ. Evaluation of two quantitative analysis methods of optical coherence tomography for detection of enamel demineralization and comparison with microhardness. Lasers Surg Med. 2014;46(9):666-71. http://dx.doi.org/10.1002/lsm.22292. PMid:25164563.

17. Quitero MFZ, Siriani LK, Azevedo CS, Freitas AZ, Scaramucci T, Simionato MRL, et al. Optical coherence tomography and polarized light microscopy for the evaluation of artificial caries: a preliminary study. Gen Dent. 2019;67(1):e1-6. PMid:30644838.

18. Almahdy A, Downey FC, Sauro S, Cook RJ, Sherriff M, Richards D, et al. Microbiochemical analysis of carious dentine using Raman and fluorescence spectroscopy. Caries Res. 2012;46(5):432-40. http://dx.doi.org/10.1159/000339487. PMid:22739587.

19. Mohanty B, Dadlani D, Mahoney D, Mann AB. Characterizing and identifying incipient carious lesions in dental enamel using micro-Raman spectroscopy. Caries Res. 2013;47(1):27-33. http://dx.doi.org/10.1159/000342432. PMid:23051625.

20. Salehi H, Terrer E, Panayotov I, Levallois B, Jacquot B, Tassery H, et al. Functional mapping of human sound and carious enamel and dentin with Raman spectroscopy. J Biophotonics. 2013;6(10):765-74. http://dx.doi.org/10.1002/jbio.201200095. PMid:22996995.

21. Timchenko V, Timchenko PE, Volova LT, Rosenbaum AY, Kulabukhova AY, Zherdeva LA, et al. Application of Raman spectroscopy method to the diagnostics of caries development. J Biomed Photonics Eng. 2015;1:201-5. http://dx.doi.org/10.18287/JBPE-2015-1-3-201.

22. Buchwald T, Okulus Z, Szybowicz M. Raman spectroscopy as a tool of early dental caries detection–new insights. J Raman Spectrosc. 2017;48(8):1094-102. http://dx.doi.org/10.1002/jrs.5175.

23. Caldwell RC, Muntz ML, Gilmore RW, Pigman W. Microhardness studies of intact surface enamel. J Dent Res. 1957;36(5):732-8. http://dx.doi.org/10.1177/00220345570360051401. PMid:13475563.

24. Vieira AE, Delbem AC, Sassaki KT, Rodrigues E, Cury JA, Cunha RF. Fluoride dose response in pH-cycling models using bovine enamel. Caries Res. 2005;39(6):514-20. http://dx.doi.org/10.1159/000088189. PMid:16251798.

25. Alkattan R, Lippert F, Tang Q, Eckert GJ, Ando M. The influence of hardness and chemical composition on enamel demineralization and subsequent remineralization. J Dent. 2018;75:34-40. http://dx.doi.org/10.1016/j.jdent.2018.05.002. PMid:29738789.

26. Zhang J, Lynch RJM, Watson TF, Banerjee A. Chitosan-bioglass complexes promote subsurface remineralisation of incipient human carious enamel lesions. J Dent. 2019;84:67-75. http://dx.doi.org/10.1016/j.jdent.2019.03.006. PMid:30951785.

27. Sorkhdini P, Crystal YO, Tang Q, Lippert F. The effect of silver diamine fluoride in preventing in vitro primary coronal caries under pH-cycling conditions. Arch Oral Biol. 2021;121:104950. http://dx.doi.org/10.1016/j.archoralbio.2020.104950. PMid:33161341.

28. Toledano M, Aguilera FS, Cabello I, Osorio R. Masticatory function induced changes, at subnanostructural level, in proteins and mineral at the resin-dentine interface. J Mech Behav Biomed Mater. 2014;39:197-209. http://dx.doi.org/10.1016/j.jmbbm.2014.07.025. PMid:25146674.

29. Stookey GK. Quantitative light fluorescence: a technology for early monitoring of the caries process. Dent Clin North Am. 2005;49(4):753-70. http://dx.doi.org/10.1016/j.cden.2005.05.009.

30. Maia AM, de Freitas AZ, de L Campello S, Gomes AS, Karlsson L. Evaluation of dental enamel caries assessment using Quantitative Light Induced Fluorescence and Optical Coherence Tomography. J Biophotonics. 2016;9(6):596-602. http://dx.doi.org/10.1002/jbio.201500111. PMid:26351155.

31. van der Veen MH, de Josselin de Jong E. Application of quantitative light-induced fluorescence for assessing early caries lesions. Monogr Oral Sci. 2000;17:144-62. http://dx.doi.org/10.1159/000061639. PMid:10949838.

32. Mujat C, van der Veen MH, Ruben JL, ten Bosch JJ, Dogariu A. Optical path-length spectroscopy of incipient caries lesions in relation to quantitative light-induced fluorescence and lesion characteristics. Appl Opt. 2003;42(16):2979-86. http://dx.doi.org/10.1364/AO.42.002979. PMid:12790448.

33. Shi XQ, Tranaeus S, Angmar-Månsson B. Comparison of QLF and DIAGNOdent for quantification of smooth surface caries. Caries Res. 2001;35(1):21-6. http://dx.doi.org/10.1159/000047426. PMid:11125192.

34. Azevedo CS, Trung LCE, Simionato MRL, Freitas AZ, Matos AB. Evaluation of caries-affected dentin with optical coherence tomography. Braz Oral Res. 2011;25(5):407-13. http://dx.doi.org/10.1590/S1806-83242011000500006. PMid:22031053.

35. Espigares J, Sadr A, Hamba H, Shimada Y, Otsuki M, Tagami J, et al. Assessment of natural enamel lesions with optical coherence tomography in comparison with microfocus x-ray computed tomography. J Med Imaging (Bellingham). 2015;2(1):014001. http://dx.doi.org/10.1117/1.JMI.2.1.014001. PMid:26158079.

36. Macey R, Walsh T, Riley P, Hogan R, Glenny AM, Worthington HV, et al. Transillumination and optical coherence tomography for the detection and diagnosis of enamel caries. Cochrane Database Syst Rev. 2021;1(1):CD013855. http://dx.doi.org/10.1002/14651858.CD013855. PMid:33502759.

37. Fried WA, Abdelaziz M, Darling CL, Fried D. High contrast reflectance imaging of enamel demineralization and remineralization at 1950-nm for the assessment of lesion activity. Lasers Surg Med. 2021;53(7):968-77. http://dx.doi.org/10.1002/lsm.23371. PMid:33442896.

38. Popescu DP, Sowa MG, Hewko MD, Choo-Smith LP. Assessment of early demineralization in teeth using the signal attenuation in optical coherence tomography images. J Biomed Opt.

2008;13(5):054053. http://dx.doi.org/10.1117/1.2992129. PMid:19021433.

39. Ramakrishnaiah R, Rehman GU, Basavarajappa S, Al Khuraif AA, Durgesh BH, Khan AS, et al. Applications of Raman spectroscopy in dentistry: analysis of tooth structure. Appl Spectrosc Rev. 2015;50(4):332-50. http://dx.doi.org/10.1080/05704928.2014.986734.

40. Min JH, Inaba D, Kwon HK, Chung JH, Kim BI. Evaluation of penetration effect of resin infiltrant using optical coherence tomography. J Dent. 2015;43(6):720-5. http://dx.doi.org/10.1016/j.jdent.2015.03.006. PMid:25862274.

41. Gutiérrez-Salazar MP, Reyes-Gasga J. Microhardness and chemical composition of human tooth. Mater Res. 2003;6(3):367-73. http://dx.doi.org/10.1590/S1516-14392003000300011.

42. Craig RG, Peyton FA. The micro-hardness of enamel and dentin. J Dent Res. 1958;37(4):661-8. http://dx.doi.org/10.1177/00220345580370041301. PMid:13563727.

43. Lippert F, Lynch RJ. Comparison of Knoop and Vickers surface microhardness and transverse microradiography for the study of early caries lesion formation in human and bovine enamel. Arch Oral Biol. 2014;59(7):704-10. http://dx.doi.org/10.1016/j.archoralbio.2014.04.005. PMid:24798979.

44. Hodge HC. Hardness tests on teeth. J Dent Res. 1936;15(5):271-9. http://dx.doi.org/10.1177/00220345350150050501.

45. Davidson CL, Hoekstra IS, Arends J. Microhardness of sound, decalcified and etched tooth enamel related to the calcium content. Caries Res. 1974;8(2):135-44. http://dx.doi.org/10.1159/000260101. PMid:4600447.

46. Gustafson G, Kling O. Micro-hardness measurements in the human dental enamel. Scand J Dent Res Odontol. Tidskr. 1948;56:23-30.

47. Meredith N, Sherriff M, Setchell DJ, Swanson SA. Measurement of the microhardness and Young's modulus of human enamel and dentine using an indentation technique. Arch Oral Biol. 1996;41(6):539-45. http://dx.doi.org/10.1016/0003-9969(96)00020-9. PMid:8937644.

48. Angmar B, Carlstrom D, Glas JE. Studies on the ultrastructure of dental enamel. IV. The mineralization of normal human enamel. J Ultrastruct Res. 1963;8(1-2):12-23. http://dx.doi.org/10.1016/S0022-5320(63)80017-9. PMid:14013184.

49. Robinson C, Weatherell JA, Hallsworth AS. Variaton in composition of dental enamel within thin ground tooth sections. Caries Res. 1971;5(1):44-57. http://dx.doi.org/10.1159/000259731. PMid:5278608.

50. Kodaka T, Debari K, Yamada M, Kuroiwa M. Correlation between microhardness and mineral content in sound human enamel (short communication). Caries Res. 1992;26(2):139-41. http://dx.doi.org/10.1159/000261498. PMid:1325874.

51. Das Gupta S, Killenberger M, Tanner T, Rieppo L, Saarakkala S, Heikkilä J, et al. Mineralization of dental tissues and caries lesions detailed with Raman microspectroscopic imaging. Analyst (Lond). 2021;146(5):1705-13. http://dx.doi.org/10.1039/D0AN01938K. PMid:33295890.

52. Shah FA. Characterization of synthetic hydroxyapatite fibers using high-resolution, polarized raman spectroscopy. Appl Spectrosc. 2021;75(4):475-9. http://dx.doi.org/10.1177/0003702820942540. PMid:32588640.

Erika Michele dos Santos Araujo
(Corresponding address)
Universidade de São Paulo, Departamento de Dentística, Faculdade de Odontologia. São Paulo, SP, Brazil
Email: erikaaraujo@alumni.usp.br

Date submitted: 2022 Apr 14
Accepted submission: 2022 Sep 27